NANO LETTERS

2007
Vol. 7, No. 9
2590−2595

In situ Raman Measurements of Suspended Individual Single-Walled Carbon Nanotubes under Strain

Sang Wook Lee,[†] Goo-Hwan Jeong,[†] and Eleanor E. B. Campbell*[,#]

Department of Physics, Göteborg University, Göteborg, SE-412 96, Sweden

Received April 14, 2007; Revised Manuscript Received July 19, 2007

ABSTRACT

We present a technique for in situ Raman measurements of suspended individual single-walled carbon nanotubes (SWNTs) under strain. We observe a strong change in the radial breathing mode intensity with increasing strain as the nanotube moves out of (or into) resonance, and for strain greater than ∼2%, there is a clear irreversible upshift in the G-mode frequencies accompanied by an increase in intensity of a broad peak at a position associated with the D mode. For lower strain, the G-mode peaks (A_1, E_1, and E_2) do not change significantly in position but change in relative intensity.

Due to their remarkable mechanical and electrical properties, carbon nanotubes (CNT) continue to be the object of intense experimental and theoretical investigation. Applications of the CNT's mechanical properties within lightweight composite materials[1] are now reaching commercial products, and efforts are proceeding to increase the Young's modulus of nanotube yarns and mats to approach the theoretical limit.[2] The mechanical and electrical properties of individual carbon nanotubes have also been the object of much fundamental interest. In recent years, CNT-based nanoelectromechanical systems[3−10] have been studied to investigate the interesting coupling of electrical and mechanical behavior that occurs on the nanoscale. The change of the electronic properties of an individual CNT as mechanical force is applied is one of the most intriguing issues within this larger topic.[4−7] Structural and electronic properties of single-walled carbon nanotubes (SWNTs) under strain have been theoretically investigated by employing different calculation methods.[11−13] Most of these theoretical studies deal with the changes of bond lengths, radii, and band gaps of specific SWNTs as a function of compressive and tensile strain. It is clear from these results that the band gap of the SWNTs can change significantly as strain is applied. This was confirmed in an experimental study of transport measurements on individual suspended SWNTs under strain.[4] Concerning structural changes, Pullen et al.[13] recently used an ab initio approach to show that there was a small, chirality-dependent, linear increase in bond length with strain, except for bonds directed along the nanotube circumference. They also predicted that the radii remain unchanged under uniaxial strain up to 6%.

Resonant Raman spectroscopy is a powerful tool to probe structural and electronic changes of SWNTs in experiment.[14] There have been several experimental studies devoted to the investigation of changes in the Raman spectra when applying pressure or strain on bundles of SWNTs.[15−19] The tangential and radial breathing modes (RBM) of SWNT bundles were shown to shift both under compressive[15,16] and tensile[17−19] force. In the case of SWNT bundles, there is the added complication of the tube−tube interaction and how it affects the Raman spectra under external forces. Cronin et al.[20,21] reported Raman studies of individual SWNTs deposited on a silicon substrate that were placed under strain by manipulating the nanotubes with an AFM tip (pushing the central part of the nanotube across the substrate) and studying the Raman spectra before and after manipulation. They observed a very clear downshift in the position of the G band which was much larger than that observed by the same group in later experiments on bundles of nanotubes where the strain was applied via an elastic polymer substrate.[19] In all of the studies reported so far, there have been interactions either between individual nanotubes or between a nanotube and a substrate, which can serve to complicate the effects. In the present work, we apply strain to individual suspended SWNTs grown between a Si cantilever and a support. The strain is applied by deflecting the cantilever with an AFM tip while simultaneously recording the Raman spectra. The results are qualitatively different from those reported by Cronin et al.[20,21]

The experiments were carried out using a combined Renishaw/Nanonics micro-Raman/AFM setup. The AFM tip

* To whom correspondence should be addressed. E-mail: Eleanor.Campbell@ed.ac.uk.
† Equal contribution to this work.
# Also at School of Chemistry, Edinburgh University, West Mains Road, Edinburgh EH9 3JJ, Scotland.

10.1021/nl070877x CCC: $37.00 © 2007 American Chemical Society
Published on Web 08/25/2007

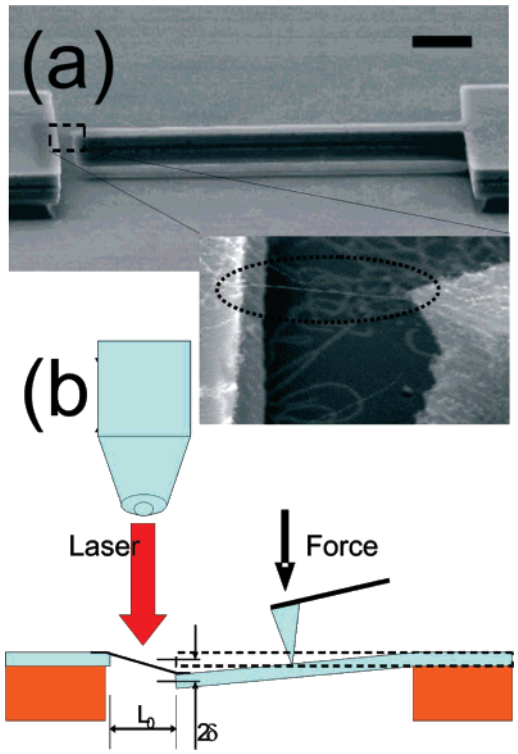

Figure 1. (a) Typical SEM image of silicon cantilever structure. Scale bar shows 10 μm. Inset: zoomed-in SEM image of individual SWNTs suspended between the end of the cantilever and the platform. (b) Schematic configuration of the setup for a strain-force-dependent in situ resonant Raman measurement. L_0 is the length of the suspended SWNT, and 2δ is the downward distance of the SWNT due to deflection of the silicon cantilever by AFM tip manipulation.

was used to deflect a Si cantilever which formed one support of a suspended SWNT, shown in Figure 1. Axial strain was applied to the nanotube by deflecting the cantilever via a force applied by the AFM tip. As was the case for the studies of nanotubes deposited on substrates, the deflection force was applied perpendicular to the nanotube axis; however, the resulting strain was primarily uniaxial.[21] In the present experiments, we could also rule out any contribution from torsional strain, which was less straightforward for the earlier studies. The micromechanical silicon cantilever structures were fabricated by selective plasma etching of Si and wet etching of SiO_2 with buffered hydrofluoric acid. The dimensions of the cantilever (70 μm long, 4 μm thick, 4 μm wide) and the counterpart support platform were defined by electron beam lithography on a silicon-on-insulator (SOI) wafer. The distance between the cantilever and the platform was typically 1−2 μm.

SWNTs were synthesized by thermal chemical vapor deposition. As-purchased ferritin solution (Sigma Aldrich) was diluted (0.01 vol %) with deionized water and deposited on the cantilever to serve as the catalyst for SWNT growth.[22] After calcination of the ferritin molecules, SWNTs were grown using methane and hydrogen gas at 900 °C for 5 min. The ferritin density was adjusted to ensure that, on average, one suspended SWNT was grown between the cantilever and the platform. Strain-force-dependent resonant Raman spectroscopy was performed on the individual suspended SWNTs by combining an AFM head (Nanonics Imaging Ltd.) with a micro-Raman measurement system (Renishaw) operated with a 514.5 nm laser. The AFM tip was placed at the center of the silicon cantilever. The cantilever was long enough to avoid the screening of the laser beam by the AFM tip since the average width of the commercially available AFM probe is around 30 μm. The spring constant of the silicon cantilever was estimated at the center by force−distance measurements with an AFM tip (spring constant of the AFM cantilever was ∼15 N/m) and found to be ∼18 N/m. From the force calibration, shown in Figure 2, we could determine a linear relationship between the deflection voltage of the AFM system and the height difference at the center of the cantilever. A deflection voltage of, for example, 0.5 V induces a 22.5 nm height difference, corresponding to a downward deflection of 45 nm at the end of the cantilever. Resonant Raman spectroscopy measurements were done while the AFM tip was pushing on the silicon cantilever. Each time the force was increased on the cantilever, the laser that monitored the deflection of the AFM tip was screened by a homemade shutter to aid focusing and also to prevent any interference with the Raman signal from the stretched SWNT. It was also possible to check the position of the end of the AFM tip when the shutter was in place, as shown in the left-side inset of Figure 2. The focus of the micro-Raman laser spot was adjusted to coincide with the suspended SWNT after the spot was located exactly in the gap space between the end of the silicon cantilever and the platform. The focus was readjusted each time after increasing the pushing force on the cantilever. As has been noted previously,[23] the Raman signal from suspended SWNTs is much stronger than the signal from SWNTs lying on the substrate, which, combined with the poor focus conditions in our experiment for the nanotubes on the substrate, means that we only detect the Raman signal from the suspended nanotube.

Figure 3a shows the strain-force dependence of the resonant Raman spectra of a suspended SWNT. The maximum strain used in this series of measurements was estimated to be ∼1%. There is some uncertainty in this value due to the uncertainty in the amount of slack present initially in the suspended nanotube and the possible influence of slippage at the high deflections. The strain values used throughout this paper are estimated assuming an initially taut nanotube and no slippage. We have carried out systematic measurements to estimate the effect of slippage. We did not observe any indication of slippage for nominal applied strain of up to ∼1%. We have also not observed any abrupt changes in the Raman spectrum for these relatively low strain values that can be attributed to slippage, as was observed by Kumar and Cronin for nanotube bundles.[19] Beyond this nominal strain value, we observed irreversible changes in the Raman spectra due to damage of the nanotubes. It is probable that a certain degree of slippage was occurring for these extreme strain values, but at present, this is difficult to quantify.

The frequencies and fwhm of the measured Raman peaks were determined by fitting the spectra assuming Lorentzian line shapes. The error bar on the experimental frequency and

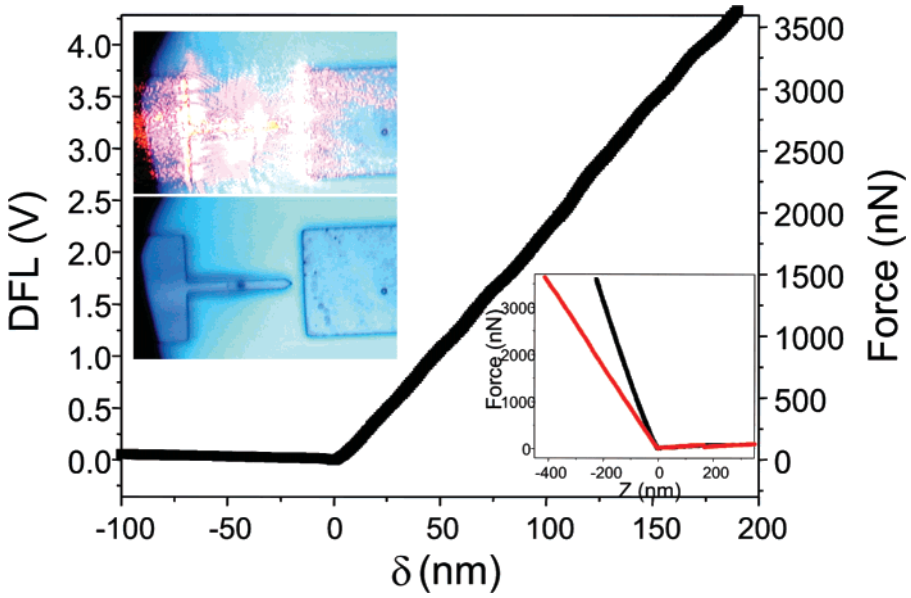

Figure 2. Force-deflection curve of a silicon cantilever. The pushing force is applied in the middle of the cantilever using AFM tip manipulation. Upper inset: optical microscope image of the device when the AFM tip pushed the cantilever (upper) before and (lower) after the shutter screened the laser from the AFM head. Lower inset: force-displacement curve measured on the cantilever (red line) and on a Si substrate (black line) for calibration of the spring constant of the cantilever.

fwhm is typically on the order of 1 cm^{-1}. The radial breathing mode is clearly seen at 169 cm^{-1}. According to the relationship given by Meyer et al.,[24] determined for free-standing SWNTs, this corresponds to a semiconducting nanotube with a diameter of 1.45 nm and is most probably an (11,10) nanotube. Examples of some fitted tangential (G-band) modes for the same nanotube are shown in Figure 3b. The Raman laser was not aligned parallel to the nanotube axis so all six allowed transitions could be observed, corresponding to transitions with A, E_1, and E_2 symmetry for both the G^+ and G^- bands. The peak positions and fwhm, determined without strain applied to the nanotube, are listed in Table 1 (SWNT1). There is an upshift/downshift ($\omega_{G^-}/\omega_{G^+}$) in the measured frequencies compared to the values reported for nanotubes of the same diameter isolated on a Si/SiO_2 substrate[25] by 3−5 cm^{-1} for the A and E_1 transitions and by +12 cm^{-1} (ω_{G^-}) and −16 cm^{-1} (ω_{G^+}) for the E_2 transitions. A similar trend is noted for the second nanotube (ω_{RBM} = 186 cm^{-1}, d = 1.28 nm, most probably (10,9)), whose values are given in Table 1 (SWNT2, spectra provided as Supporting Information). All six Lorentzians are needed to obtain a good fit to the data, although the E_2 transitions are typically lower in intensity than the A and E_1 transitions. The fitted line widths are consistent with the natural line widths of the transitions.[26] In addition to the sharp peaks, it is also necessary (in particular for high strain) to fit broad features at ∼1540 (fwhm ca. 100 cm^{-1}) and 1610 cm^{-1} (fwhm ca. 60 cm^{-1}). These features have been noted previously in weakly resonant G-band spectra from semiconducting SWNTs and associated with a double-resonance process.[14,25,27] We observe that the broad features are more intense in spectra with small radial breathing mode intensities, that is, for tubes that are only weakly resonant, in agreement with previous observations.

Some clear tendencies can be observed in the strain-dependent measurements. The radial breathing mode frequency does not shift with increasing strain within our experimental uncertainty. This is in agreement with recent calculations[13] and with the experimental study of individual strained nanotubes on a substrate by Cronin et al.[20] However, in contrast to the study of Cronin et al., we do observe a clear change in the intensity of the radial breathing mode transition. This is shown in more detail in Figure 4 where the integrated RBM peak intensities are plotted as a function of the AFM deflection voltage (and estimated strain). Two sets of data are shown here. Figure 4a corresponds to the spectra shown in Figure 3 and Figure 4b to the results from SWNT2. The strain applied to the nanotube can be estimated according to the approximate relation strain [%] = B × voltage^2, with B = 0.1 for SWNT1 (length = 2 μm) and B = 0.4 for SWNT2 (length = 1 μm). For SWNT1, which initially showed an intense RBM signal, the intensity falls off linearly with increasing strain until it disappears completely for AFM deflection voltages greater than 2.5 V (estimated strain > 0.6%). For SWNT2, which initially showed a very weak RBM peak (indicating only weak resonance), the RBM intensity first increases as strain is applied, reaching a maximum for a strain of approximately 0.4%, and then decreases toward zero. This can be explained in terms of the deformation of the electronic band structure with the application of strain.[13,17] The experimental resonance window for the RBM of isolated, suspended nanotubes is on the order of 8 meV.[28] Band gap changes significantly larger than this can be expected for the strains applied in the present experiments.[4,13] The overall intensity of the G band does not change so dramatically (the resonance window is much less critical for the G peaks since the phonon energy is larger[28]), but a close look at the spectra in Figure 3 shows

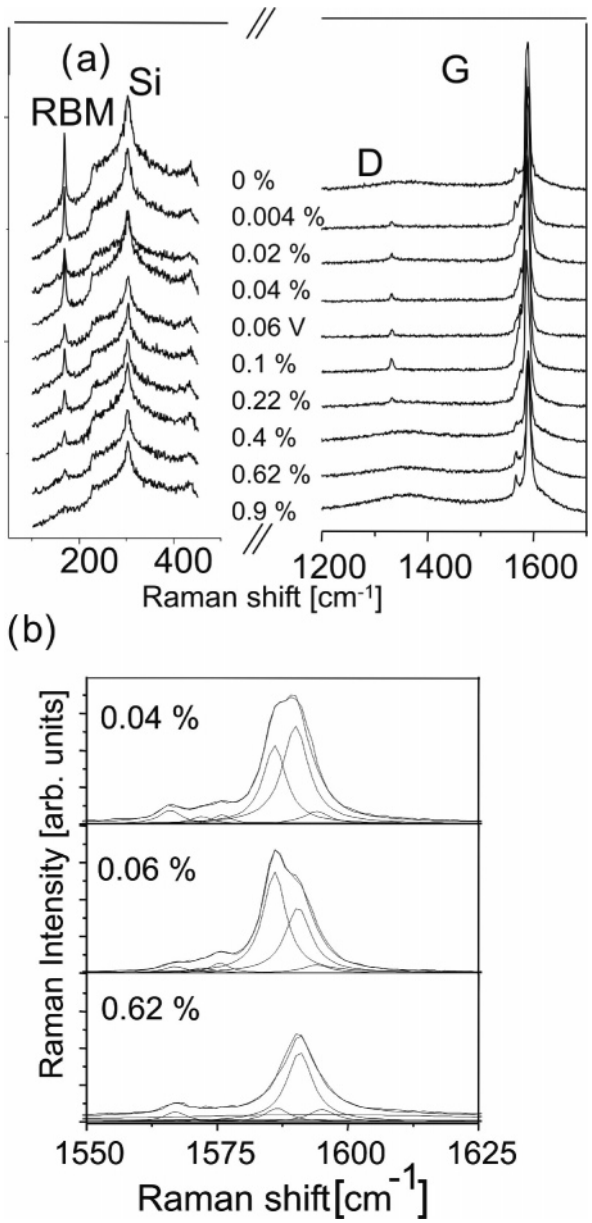

Figure 3. Deflection-force-dependent in situ resonance Raman spectroscopy result on a suspended individual SWNT. (a) Change of Raman spectra depending on AFM deflection voltage (lower *x*-axis) and estimated strain (upper *x*-axis) from 0.0 to 3.0 V. (b) G-band peak fits for three different values of the estimated strain.

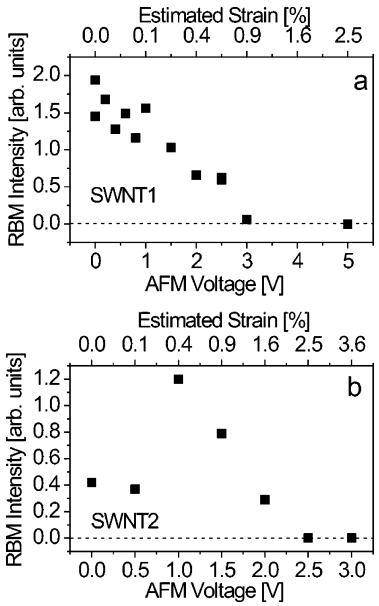

Figure 4. Integrated radial breathing mode (RBM) intensity as a function of AFM deflection voltage (lower *x* axis) and estimated strain (upper *x* axis) for (a) SWNT1 and (b) SWNT2.

that the relative intensities of the A and E_1 peaks of the G^+ band undergo strong changes as strain is applied. This behavior has been found to be strongly dependent on the individual nanotube, with some nanotubes showing relatively little change in relative intensities for a similar nominal strain range. However, the changes in the relative intensities for a given individual nanotube are reproducible and reversible. Figure 5 shows that the G^+ A/E_1 ratio for SWNT1 reaches a minimum for AFM deflection voltages in the range of 0.4−1.5 V (ca. 0.16−0.22% strain) before rapidly increasing again to a maximum at 2.5 V (0.6% strain). Interestingly, the minimum in the G^+ A/E_1 ratio is accompanied by the appearance of a small, narrow peak at the position of the D mode (1333 cm^{-1}, fwhm 5 cm^{-1}). Such behavior is not observed for every nanotube, and we assume that it is related to a resonant process with a relatively narrow resonance window. Detailed ab initio calculations are required to elucidate the mechanisms for these changes, but it is clear from these spectra that strain measurements on suspended nanotubes have the potential to provide a very stringent test of theoretical studies of the electronic structure and transition matrix elements of individual nanotubes.

The G-band peak positions are plotted in Figure 6 as a function of the applied strain for SWNT1 (Figure 5a) and SWNT2 (Figure 5b). In contrast to the study of Cronin et al. for nanotubes deposited on a substrate,[20,21] we do not observe any down-shift in the frequencies of the G-band transitions. For both nanotubes, we observe an increase in the frequencies as the strain is increased beyond a certain critical value (ca. 2% in both cases). This effect is more apparent for SWNT2 (Figure 5b), which is exposed to higher strain and where it is also possible to see that the frequency shift is larger for the G^- peaks than that for the G^+ peaks.

Table 1. Fitted Lorentzian Peak Positions and fwhm for Two Suspended SWNTs without the Application of Strain; the Diameter Has Been Calculated Using the Expression Given by Meyer et al.,[24] ω_{RBM} [cm^{-1}] = 204/*d* [nm] + 27

	RBM	diam.	G^- A	G^- E_1	G^- E_2	G^+ A	G^+ E_1	G^+ E_2
SWNT1, ω	169	1.45 nm	1572	1576	1566	1590	1586	1594
SWNT1, fwhm	5		5	4	5	6	5.3	6
SWNT2, ω	186	1.28 nm	1568	1575	1563	1590.5	1586	1595
SWNT2, fwhm	7		7	7	7	6	5.3	6

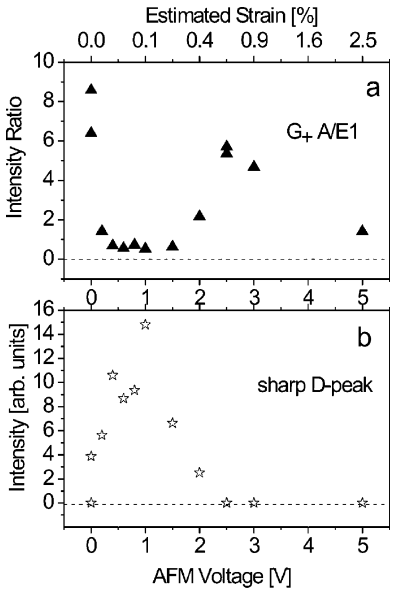

Figure 5. (a) Ratio of integrated A/E_1 peak intensities (triangles and left-hand *y* axis) and (b) the integrated sharp (1333 cm^{-1}, fwhm 5 cm^{-1}) D-peak intensity (stars, right-hand axis) as a function of AFM deflection voltage (lower *x* axis) and estimated strain (upper *x* axis). The integrated peak intensities were normalized to the Si peak intensity for each spectrum.

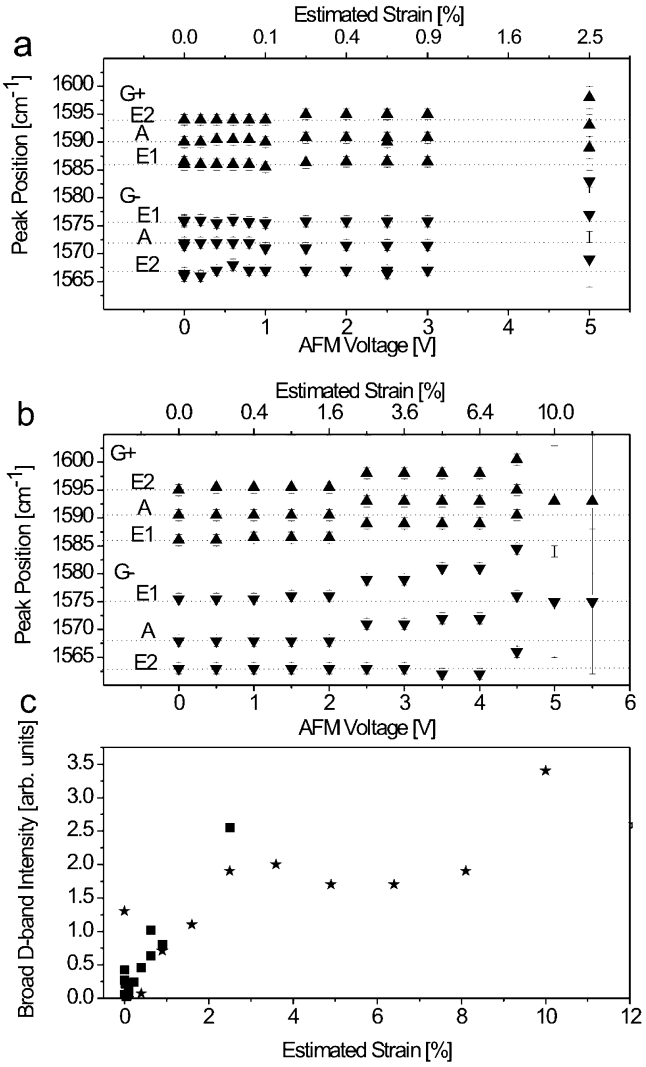

Figure 6. (a) G-mode peak positions as a function of AFM deflection voltage (lower *x* axis) and strain (upper *x* axis) for SWNT1. (b) G-mode peak positions as a function of AFM deflection voltage (lower *x* axis) and strain (upper *x* axis) for SWNT2. The large error bars for 5 and 5.5 V indicate that the individual peaks could not be clearly resolved, and both the G^+ and G^- bands were each fitted with a single Lorentzian. The dotted lines mark the initial position of the peak for zero applied strain and are simply to aid the eye. (c) Integrated broad D-mode intensity (1367 cm^{-1}, fwhm 200 cm^{-1}) as a function of estimated strain for SWNT1 (squares) and SWNT2 (stars).

For an applied AFM deflection voltage of 5 V or higher on SWNT2 ($\geq$10% strain), it was not possible to resolve the individual peaks and, only two Lorentzians were used to fit the data instead of six. Once we observed this shift in the G-peak frequencies, the spectral changes were no longer reversible. We therefore attribute the change in the frequencies to the occurrence of damage in the nanotubes.

In addition to the small, sharp D peak visible in the spectra shown in Figure 3a, there is a much broader peak centered at 1367 cm^{-1} (independent of applied strain) with a fwhm of 200 cm^{-1}. This becomes clearly visible for large strain and is observed in both sets of spectra (SWNT1 and SWNT2). The integrated peak intensities for both nanotubes are plotted in Figure 6c as a function of AFM deflection voltage. We often observe a small, finite, broad peak intensity for zero force applied to the silicon cantilever, which then disappears for low values of strain (up to ca. 1%) before increasing strongly as the strain is increased beyond this value. Such behavior can be clearly seen in Figure 6c for both samples. The finite peak intensity for zero force may be related to initial slack in the suspended nanotube, although this is too small to be observed by SEM. Alternatively, it is conceivable that the application of a small strain can help heal some intrinsic defects in the nanotube.

In summary, we have measured in situ Raman spectroscopy of suspended individual SWNTs under strain. The position of the radial breathing mode frequency remains constant as strain is increased, but the intensity changes due to the modification of the band structure, leading to a change in the resonance conditions. This observation is in agreement with calculations for semiconducting nanotubes.[13,17,21] The results concerning the G-mode peaks are more unexpected. One would intuitively expect that an increase in nanotube length would lead to a corresponding increase in the bond length in the axial direction and hence to an expected decrease in frequency. A large down-shift was also observed in earlier experimental work.[20,21] However, in the present experiments, the positions of the G-mode peaks do not change significantly until the strain exceeds $\sim$2%, when one can observe an upshift in the frequency. These changes to the spectra are irreversible and indicate that structural changes have occurred. The effect is most pronounced for the G^- peaks. Below this, although the peak positions remain constant, there can be strong variations in the relative peak intensities both for the G mode and the D mode. These changes are reversible and are attributed to changes in the band structure affecting the resonance conditions. Both

nanotubes that we studied in detail in the present paper are very close to the armchair in geometries (11,10) and (10,9). We would therefore not expect a significant shift in the frequencies of the transverse G^- peaks, in agreement with our experimental observations, since the relevant bond lengths would not be significantly effected by the appliance of axial strain. However, we would still expect the longitudinal G^+ peaks to shift downward. Reich et al.[29] carried out full ab initio calculations on two chiral nanotubes and showed that chiral tubes yield qualitatively and quantitatively different results from achiral ones, with evidence for a strong mixing of the optical modes. The situation is therefore considerably more complex than might be assumed from tight-binding calculations, and we hope that our present results might stimulate more theoretical studies into the properties of chiral nanotubes.

In addition to the sharp Lorentzian peaks that have a fwhm close to the natural line width, there are also broad peaks associated with the G mode and D mode. These broad signals do not change position but increase significantly in intensity when the strain is increased beyond ~0.5%. The broad G-mode peaks have been noted previously and associated with double-resonance features. The broad D-mode peak may be associated with the introduction of defects in the nanotube structure under high strain.

The results that we present here show quite significant differences when compared with earlier measurements made on nanotubes lying on a substrate[20,21] and illustrate the importance of systematic experimental studies of freely suspended nanotubes accompanied by theoretical studies to elucidate the complicated processes involved as nanotubes are subjected to outside forces. Our measurement scheme has considerable potential for the study of the intrinsic structural and electronic properties of one-dimensional nanostructures under strain, such as SWNTs, double-walled CNT, and other one-dimensional nanowires.

Acknowledgment. This work is supported by Vetenskapsrådet, SSF, and STINT. One of the authors (S.W.L.) is partially supported by the Korea Research Foundation Grant funded by the Korean Government (MOEHRD) (KRF-2005-214-C00198). The authors thank H. Brenning and B. S. Kang for their help in preparing the Si cantilever structure and with SEM observations.

Supporting Information Available: Full waterfall plots for the Raman data obtained for SWNT2 and reversibilty test results. This material is available free of charge via the Internet at http://pubs.acs.org. results

References

(1) Barrera, E. V.; Shofner, M. L.; Corral, E. L. In *Carbon Nanotubes Science and Applications*; Meyyappan, M., Ed.; CRC Press: Boca Raton, FL, 2005; Chapter 11.
(2) Zhang, M.; Fang, S. L.; Zakhidov, A. A.; Lee, S. B.; Aliev, A. E.; Williams, C. D.; Atkinson, K. R.; Baughman, R. H. *Science* **2005**, *309* 1215.
(3) Williams, P. A.; Papadakis, S. J.; Patel, A. M.; Falvo, M. R.; Washburn, S.; Superfine, R. *Phys. Rev. Lett.* **2002**, *89*, 255502.
(4) Cao, J.; Wang, Q.; Dai, H. *Phys. Rev. Lett.* **2003**, *90*, 157601.
(5) Minot, E. D.; Yaish, Y.; Sazonova, V.; Park, J.-Y.; Brink, M.; McEuen, P. L. *Phys. Rev. Lett.* **2003**, *90*, 156401.
(6) Meyer, J. C.; Paillet, M.; Roth, S. *Science* **2005**, *309*, 1539.
(7) Sazonova, V.; Yaish, Y.; Üstünel, H.; Roundy, D.; Arias, T. A.; McEuen, P. L. *Nature* **2004**, *431*, 284.
(8) Fennimore, A. M.; Yuzvinsky, T. D.; Han, W.-Q.; Fuhrer, M. S.; Cumings, J.; Zettl, A. *Nature* **2003**, *424*, 408.
(9) Lee, S. W.; Lee, D. S.; Morjan, R. E.; Jhang, S. H.; Sveningsson, M.; Nerushev, O.; Park, Y. W.; Campbell, E. E. B. *Nano Lett.* **2004**, *4*, 2027.
(10) Kim, P.; Lieber, C. M. *Science* **1999**, *286*, 2148.
(11) Yang, L.; Han, J. *Phys. Rev. Lett.* **2000**, *85*, 154.
(12) Sears, A.; Batra, R. C. *Phys. Rev. B* **2004**, *69*, 235406.
(13) Pullen, A.; Zhao, G. L.; Bagayoko, D.; Yang, L. *Phys. Rev. B* **2005**, *71*, 205410.
(14) Dresselhaus, M. S.; Dresselhaus, G.; Saito, R.; Jorio, A. *Phys. Rep.* **2005**, *409*, 47.
(15) Merlen, A.; Bendiab, N.; Toulemonde, P.; Aouizerat, A.; San Miguel, A. *Phys. Rev. B* **2005**, *72*, 035409.
(16) Venkateswaran, U. D.; Rao, A. M.; Richter, E.; Menon, M.; Rinzler, A.; Smalley, R. E.; Eklund, P. C. *Phys. Rev. B* **1999**, *59*, 10928.
(17) Lucas, M.; Young, R. J. *Phys. Rev. B* **2004**, *69*, 085405.
(18) Jiang, C.; Ko, H.; Tsukruk, V. V. *Adv. Mater.* **2005**, *17*, 2127.
(19) Kumar, R.; Cronin, S. B. *Phys. Rev. B* **2007**, *75*, 155421.
(20) Cronin, S. B.; Swan, A. K.; Ünlü, M. S.; Goldberg, B. B.; Dresselhaus, M. S.; Tinkham, M. *Phys. Rev. Lett.* **2004**, *93*, 167401.
(21) Cronin, S. B.; Swan, A. K.; Ünlü, M. S.; Goldberg, B. B.; Dresselhaus, M. S.; Tinkham, M. *Phys. Rev. B* **2005**, *72*, 035425.
(22) Jeong, G.-H.; Suzuki, S.; Kobayashi, Y.; Yamazaki, A.; Yoshimura, H.; Homma, Y. *J. Appl. Phys.* **2005**, *98*, 124311.
(23) Kobayashi, Y.; Yamashita, T.; Ueno, Y.; Niwa, O.; Homma, Y.; Ogino, T. *Chem. Phys. Lett.* **2004**, *386*, 153.
(24) Meyer, J. C.; Paillet, M.; Michel, T.; Moreac, A.; Neumann, A.; Duesberg, G. S.; Roth, S.; Sauvajol, J.-L. *Phys. Rev. Lett.* **2005**, *95*, 217401.
(25) Jorio, A.; Pimenta, M. A.; Souza Filho, A. G.; Samsonidze, G. G.; Swan, A. K.; Ünlü, M. S.; Goldberg, B. B.; Saito, R.; Dresselhaus, G.; Dresselhaus, M. S. *Phys. Rev. Lett.* **2003**, *90*, 107403.
(26) Jorio, A.; Fantini, C.; Dantas, M. S. S.; Pimenta, M. A.; Souza Filho, A. G.; Samsonidze, G. G.; Brar, V. W.; Dresselhaus, G.; Dresselhaus, M. S.; Swan, A. K.; Ünlü, M. S.; Goldberg, B. B.; Saito, R. *Phys. Rev. B* **2002**, *66*, 115411.
(27) Maultzsch, J.; Reich, S.; Thomsen, C. *Phys. Rev. B* **2002**, *65*, 233402.
(28) Jorio, A.; Souza Filho, A. G.; Dresselhaus, G.; Dresselhaus, M. S.; Saito, R.; Hafer, J. H.; Lieber, C. M.; Matinaga, F. M.; Dantas, M. S. S.; Pimenta, M. A. *Phys. Rev. B* **2001**, *63*, 245416.
(29) Reich, S.; Thomsen, C.; Ordejon, P. *Phys. Rev. B* **2001**, *64*, 195416.

NL070877X